

See discussions, stats, and author profiles for this publication at: <https://www.researchgate.net/publication/259585925>

# Formation of a Room Temperature Stable Fe–V(O) Complex: Reactivity Toward Unactivated C–H Bonds

ARTICLE in JOURNAL OF THE AMERICAN CHEMICAL SOCIETY · JANUARY 2014

Impact Factor: 12.11 · DOI: 10.1021/ja412537m · Source: PubMed

CITATIONS

25

READS

137

8 AUTHORS, INCLUDING:



**Munmun Ghosh**

CSIR - National Chemical Laboratory, Pune

6 PUBLICATIONS 47 CITATIONS

SEE PROFILE



**Chakadola Panda**

Technische Universität Berlin

10 PUBLICATIONS 106 CITATIONS

SEE PROFILE



**Andrew C Weitz**

Carnegie Mellon University

11 PUBLICATIONS 85 CITATIONS

SEE PROFILE

# Formation of a Room Temperature Stable $\text{Fe}^{\text{V}}(\text{O})$ Complex: Reactivity Toward Unactivated C–H Bonds

Munmun Ghosh,<sup>†</sup> Kundan K. Singh,<sup>†</sup> Chakadola Panda,<sup>†</sup> Andrew Weitz,<sup>§</sup> Michael P. Hendrich,<sup>§</sup> Terrence J. Collins,<sup>‡,§</sup> Basab B. Dhar,<sup>\*,†</sup> and Sayam Sen Gupta<sup>\*,†</sup>

<sup>†</sup>Chemical Engineering Division, CSIR-National Chemical Laboratory, Dr. Homi Bhabha Road, Pune, Maharashtra 411008, India

<sup>‡</sup>Institute for Green Science, <sup>§</sup>Department of Chemistry, Carnegie Mellon University, 4400 Fifth Avenue, Pittsburgh, Pennsylvania 15213, United States

## S Supporting Information

**ABSTRACT:** An  $\text{Fe}^{\text{V}}(\text{O})$  complex has been synthesized from equimolar solutions of  $(\text{Et}_4\text{N})_2[\text{Fe}^{\text{III}}(\text{Cl})(\text{biuret-amide})]$  and *m*CPBA in  $\text{CH}_3\text{CN}$  at room temperature. The  $\text{Fe}^{\text{V}}(\text{O})$  complex has been characterized by UV–vis, EPR, Mössbauer, and HRMS and shown to be capable of oxidizing a series of alkanes having C–H bond dissociation energies ranging from 99.3 kcal mol<sup>−1</sup> (cyclohexane) to 84.5 kcal mol<sup>−1</sup> (cumene). Linearity in the Bell–Evans–Polanyi graph and the finding of a large kinetic isotope effect suggest that hydrogen abstraction is engaged the rate-determining step.

High valent iron-oxo intermediates play key roles in enzymatic oxidations.<sup>1–5</sup> For example, in the cytochrome P450 enzymes, the high valent  $\text{Fe}^{\text{IV}}(\text{O})(\text{porphyrin-radical-cation})$ , isoelectronic with  $\text{Fe}^{\text{V}}(\text{O})$ , has been shown to be the reactive intermediate in the selective hydroxylation of camphor.<sup>2,6</sup> In the Rieske dioxygenase enzyme family,<sup>1</sup> an  $\text{Fe}^{\text{V}}(\text{O})$  active intermediate has been proposed.<sup>7,8</sup> Several functional models of both heme<sup>9</sup> and nonheme<sup>10–13</sup> iron-dependent monooxygenase enzymes have been synthesized<sup>15–18</sup> including the TAML system, which has provided fully functional, small molecule replicas of the peroxidase and short-circuited P450 enzymes.<sup>12,13</sup> For nonheme iron catalyzed oxidations,  $\text{Fe}^{\text{IV}}=\text{O}$  active intermediates have been isolated and structurally characterized and their reactivity toward C–H bond hydroxylation has been studied in detail.<sup>9,14–16</sup> Synthetic functional models of Rieske dioxygenase family of enzymes have been postulated to engage an  $\text{Fe}^{\text{V}}(\text{O})$  reactive species in C–H and C=C bond oxidations.<sup>17,18</sup> Several complexes having  $\text{Fe}^{\text{V}}(\text{O})$  have been reported, and they are thermally not stable above  $-40^\circ\text{C}$ .<sup>19,20</sup> Que et al. has described the formation of an  $\text{Fe}^{\text{V}}(\text{O})$  complex from  $[\text{Fe}^{\text{IV}}(\text{O})(\text{TMC})(\text{MeCN})]^{2+}$  at  $-44^\circ\text{C}$  ( $t_{1/2} = 60$  min).<sup>21</sup> Recently, Costas et al. has reported formation of a purported  $\text{Fe}^{\text{V}}(\text{O})$  at  $-60^\circ\text{C}$  (characterized using mass spectroscopy) and studied its reactivity.<sup>18</sup> Collins et al. first produced a nonheme  $\text{Fe}^{\text{V}}(\text{O})$  complex by oxidation of an  $\text{Fe}^{\text{III}}$ -TAML complex at  $-60^\circ\text{C}$  using *m*-chloroperbenzoic acid (*m*CPBA); this was thoroughly characterized by UV–vis, ESI–MS, EPR, EXAFS, and Mössbauer spectroscopies.<sup>22</sup> The  $\text{Fe}^{\text{V}}(\text{O})$  intermediate was shown to be reactive toward sulfoxidation and epoxidation in the  $-40$  to  $-60^\circ\text{C}$  range in nitrile solvents.<sup>22,23</sup> However, to

date it has not been possible to characterize and explore the ambient conditions for the reactivity of an  $\text{Fe}^{\text{V}}(\text{O})$  complex because no system has been stable enough to permit this. The availability of an  $\text{Fe}^{\text{V}}(\text{O})$  complex that is both stable and reactive at ambient to physiological temperatures would have the potential to advance insight into enzymatic oxidation processes and especially oxidations of the C–H bonds of unactivated alkanes, which are among the most difficult of all oxidation processes to carry out in a controlled fashion.

We have recently reported the first preparation and initial studies of an  $\text{Fe}^{\text{III}}$  complex of a biuret-amide based macrocyclic ligand, **1**,<sup>24a</sup> a member of the broad suite of catalysts called TAML activators that were invented by Collins in the mid-1990s.<sup>24b</sup> Complex **1** is the first member of a fifth generation of TAML activators—generation numbers mark the order of preparation of sets of TAML activators with distinctive structural motifs. Activator **1** differs from the prototypical first generation TAML activator by substitution of the  $\text{CMe}_2$  moiety in the six-membered macrocyclic subring<sup>25</sup> with an  $-\text{NMe}$  group (Figure 1). The planar six-membered ring allows

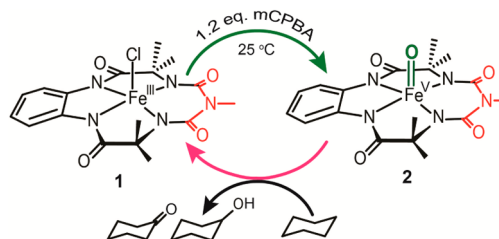


**Figure 1.** Schematic presentation of  $\text{Fe}^{\text{V}}(\text{O})$  formation and reaction toward cyclohexane.

electron donation from  $-\text{NMe}$  group and subsequent delocalization of the electron density throughout the ring.<sup>26</sup> This is evident in electrochemical studies where the  $\text{Fe}^{\text{IV}}/\text{Fe}^{\text{III}}$  couple of **1** is 230 mV higher<sup>24a</sup> than the corresponding  $\text{Fe}$ -TAML. This in addition to the fact that the  $-\text{NMe}$  group is situated far away from the Fe center made us to believe that  $\text{Fe}^{\text{V}}(\text{O})$  complex (**2**) should have stability at temperatures higher than  $-40^\circ\text{C}$ .<sup>22,23</sup> In this article, we report the formation and characterization of the  $\text{Fe}^{\text{V}}(\text{O})$  complex **2** from **1**.

**Received:** December 10, 2013

Remarkably, **2** is sufficiently stable that it can be produced quantitatively and its reactivity can be examined at room temperature. We also demonstrate that **2** readily cleaves the unactivated alkane C–H bond of cyclohexane; studies of the kinetics lead to the conclusion that H atom abstraction by  $\text{Fe}^{\text{V}}(\text{O})$  is the rate determining step (r.d.s) in the resulting hydroxylation process (Figure 1).

Complex **2** was prepared at 25 °C from the parent TAML activator,  $(\text{Et}_4\text{N})_2[\text{Fe}^{\text{III}}(\text{Cl})(\text{biuret-amide})]$  **1**, in  $\text{CH}_3\text{CN}$  by adding equimolar amounts of *m*CPBA.<sup>22</sup> Addition of 0.5 equivalent of *m*CPBA ( $5 \times 10^{-5}$  M) to **1** ( $10^{-4}$  M) at RT in  $\text{CH}_3\text{CN}$  with exclusion of  $\text{O}_2$  afforded a violet-colored solution. Addition of a second half equivalent of *m*CPBA to this violet solution resulted in the formation of a green solution with distinct absorption maxima at 441 nm ( $\epsilon = 4.35 \times 10^3 \text{ M}^{-1} \text{ cm}^{-1}$ ) and 613 nm ( $\epsilon = 3.42 \times 10^3 \text{ M}^{-1} \text{ cm}^{-1}$ ) (Figure 2A).

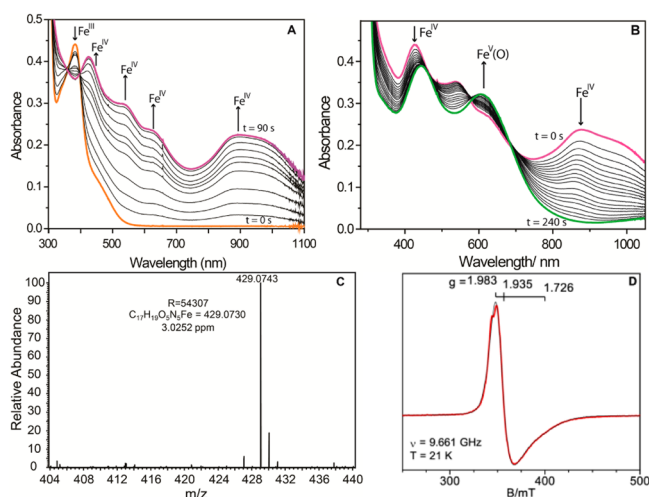


**Figure 2.** (A) UV–vis spectral changes upon addition of 0.5 equiv of *m*CPBA ( $5 \times 10^{-5}$  M) to **1** ( $10^{-4}$  M). Orange = spectrum of **1**, violet = proposed  $(\text{Fe}^{\text{IV}})_2\text{O}$  dimeric product. (B) UV–vis spectral changes upon addition of 0.5 equiv *m*CPBA ( $5 \times 10^{-5}$  M) to the preformed  $(\text{Fe}^{\text{IV}})_2\text{O}$ . Green = spectrum of  $\text{Fe}^{\text{V}}(\text{O})$ . (C) HRMS spectra of green  $\text{Fe}^{\text{V}}(\text{O})$ . (D) EPR spectra. Red =  $\text{Fe}^{\text{V}}(\text{O})$ , Blue = simulated spectrum.

The green solution was examined by mass, EPR, and Mössbauer spectroscopies. A sample of the green solution was split and frozen in liquid nitrogen and then analyzed with EPR and Mössbauer spectroscopies. The X-band EPR spectrum at 21 K showed a rhombic  $S = 1/2$  species with  $g = 1.983, 1.935, 1.726$  (Figure 2D). Spin quantification indicated quantitative conversion of the starting  $\text{Fe}^{\text{III}}$  complex (**1**) to the corresponding  $\text{Fe}^{\text{V}}(\text{O})$  (**2**). The Mössbauer spectrum of  $^{57}\text{Fe}$  enriched **2** at 4 K showed a doublet with an isomer shift of  $\Delta = -0.44 \text{ mm/s}$  and quadrupole splitting of  $\Delta E_Q = 4.27 \text{ mm/s}$  (Supporting Information Figure SI 1). A paramagnetic pattern is not observed, and the doublet is broad due to intermediate relaxation of the spin system. The intermediate relaxation and broad EPR signal suggest molecular aggregation. The  $g$ -values and Mössbauer parameters are close to those of the  $\text{Fe}^{\text{V}}(\text{O})$  complex reported previously.<sup>22</sup> Both the EPR and Mössbauer spectral analyses suggest quantitative conversion ( $\geq 95\%$ ) of the starting **1** to **2** (Figure 2 and Supporting Information Figure SI 1). This is in contrast to the  $\text{Fe}^{\text{V}}(\text{O})$  prototype TAML, where only 70% of  $\text{Fe}^{\text{V}}$  was produced from the starting  $\text{Fe}^{\text{III}}$  complexes at  $-40$  °C (by Mössbauer spectroscopy).<sup>22</sup> HRMS examination of **2** in  $\text{CH}_3\text{CN}$  revealed one prominent ion at a

mass-to-charge ratio of 429.0745 (calculated  $m/z$  429.0730); the isotopic distribution pattern corresponded to that expected for **2** (Figure 2C). HRMS analysis of a solution prepared by introduction of  $\text{H}_2^{18}\text{O}$  ( $0.5 \mu\text{L}$ ) into the solvent media during the synthesis of **2** showed 70% formation of  $\text{Fe}^{\text{V}}(^{18}\text{O})$  ( $m/z$  431.078, Supporting Information Figure SI 2).

Addition of 1 equiv of **1** to **2** also resulted in formation of a violet solution, the UV–vis spectrum (Figure 2A) of which was identical to the solution formed by addition of 0.5 equiv of *m*CPBA to **1**. This common UV–vis spectrum with its conspicuous features at long wavelengths was very similar to the known UV–vis spectra of  $\mu$ -oxo- $(\text{Fe}^{\text{IV}})_2$  species of established Fe-TAML complexes.<sup>23,27</sup> Moreover, the violet solution was found to be EPR silent. Because they were diamagnetic, their  $^1\text{H}$  NMR spectra was recorded (Supporting Information Figure SI 3), which again reproduced the behavior of the parent  $(\text{Fe}^{\text{IV}})_2\text{O}$  TAML complexes.<sup>27</sup> The rate of comproportionation between **1** and **2** was determined to be  $1.00 \times 10^5 \text{ M}^{-1} \text{ s}^{-1}$ , twice the rate of the corresponding process for the prototype TAML (NMe replaced by  $\text{CMe}_2$ , Supporting Information Figure SI 4), consistent with the less sterically encumbered nature of the biuret system.<sup>23</sup> A detailed study to elucidate the nature of this  $\text{Fe}^{\text{IV}}$  is currently underway.

The spontaneous reduction of  $\text{Fe}^{\text{V}}$  to  $\text{Fe}^{\text{IV}}/\text{Fe}^{\text{III}}$  was studied using UV–vis spectroscopy by monitoring the decrease characteristic 613 nm band of **2**. The initial rate of the decay was found to be first order with respect to **2** and the first order rate constants for the decay ( $k_{5/4,3}$ ) were determined from the slope of the straight lines at three different temperatures of 25, 10, and 4 °C (Supporting Information Figure SI 5). The  $k_{5/4,3}$  value at 25 °C ( $4.45 \times 10^{-5} \text{ s}^{-1}$ ) was similar to the  $\text{Fe}^{\text{V}}(\text{O})$  prototype TAML reported at  $-40$  °C,<sup>23</sup> showing that the biuret-substituted TAML ligand leads to a much more stable  $\text{Fe}^{\text{V}}(\text{O})$  complex. In fact, **2** is the first example of an  $\text{Fe}^{\text{V}}(\text{O})$  complex that is stable at room temperature. The stability of the  $\text{Fe}^{\text{IV}}$  species (generated by reaction of **1** with 0.5 equivalent of *m*CPBA) was determined by monitoring the decrease of a characteristic band at 428 nm. Over time, this proposed  $(\text{Fe}^{\text{IV}})_2\text{O}$  slowly converted to **1**.

The unprecedented high stability of **2** has allowed us to examine its room temperature reactivity. Activation of C–H bonds by **2** at room temperature were studied for a range of hydrocarbons with bond dissociation energies (BDE), spanning 85–100  $\text{kcal mol}^{-1}$ .<sup>28</sup> Excess cyclohexane (1000 equiv) was added to a solution of **2** ( $10^{-4}$  M) in  $\text{CH}_3\text{CN}$  at 25 °C with exclusion of  $\text{O}_2$ , and the reaction was monitored by UV–vis spectroscopy. Upon addition of cyclohexane, spectral scans showed the rapid formation of a mixture of  $\text{Fe}^{\text{IV}}$  and  $\text{Fe}^{\text{III}}$  species, which then slowly converted to **1** (ESI–MS, UV–vis confirmation, Figure 3). GC and GC–MS analysis indicated cyclohexanol and cyclohexanone as products (Table 1), showing **2** is capable of effective oxygen atom insertion into an unactivated C–H bond. Based on the concentration of **2**, the yield of the reaction was determined to be 42% with an alcohol to ketone ratio of 9:1 (Table 1, Supporting Information Figures SI 6 and SI 7). Reactions of **2** with substrates having stronger and weaker C–H bonds than cyclohexane were also studied. Addition of benzene (BDE of C–H  $\sim 110 \text{ kcal mol}^{-1}$ ) to a solution of **2** showed no additional change in the UV–vis spectrum and no product was observed by GC–MS. In contrast, substrates having lower BDE like cumene, ethylbenzene, toluene, and 2,3-dimethylbutane (DMB) reacted more rapidly with **2** than with cyclohexane. In the case of

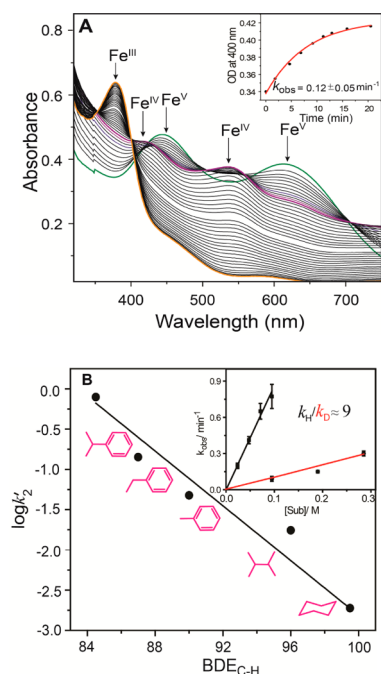


**Figure 3.** (A) UV-vis spectral changes upon reaction of **2** ( $1 \times 10^{-4}$  M) with cyclohexane (0.093 M). (Inset) the absorbance vs time plot at 400 nm (■ indicates experimental data point; the red line is the first order fit according to the equation  $[A_t = A_\infty - (A_\infty - A_0)e^{-(k_{\text{obs}}t)}]$ ). (B)  $\log k_2'$  vs  $\text{BDE}_{\text{C-H}}$  of various hydrocarbons for the reactions with **2** at 25 °C. (Inset) Plot of  $k_{\text{obs}}/\text{min}^{-1}$  vs [toluene] (black line) and [toluene- $d_8$ ] (red line) showing a pronounced KIE at 25 °C.

DMB, **2** selectively hydroxylated the tertiary C–H bond ( $\text{BDE} \sim 96 \text{ kcal mol}^{-1}$ , Table 1) in preference to the primary C–H bond ( $\text{BDE} \sim 99 \text{ kcal mol}^{-1}$ ), leading exclusively to the formation of 2,3-dimethyl-2-butanol.

To confirm, if part of the product obtained was due to the reaction with the  $\text{Fe}^{\text{IV}}$  species, which is initially formed upon addition of substrate to **2**, the reactivity of the  $\text{Fe}^{\text{IV}}$  species (generated by the reaction of complex **1** with 0.5 equiv of *m*CPBA) toward C–H activation was also explored. It was found from UV-vis, GC, and GC-MS studies that the reaction of cyclohexane with  $\text{Fe}^{\text{IV}}$  species did not lead any product formation on the time scale ( $\geq 6 \text{ h}$ ) of the experiments.

Extensive kinetic studies were performed to ascertain the nature of the hydroxylations by **2** using UV-vis spectroscopy at the isosbestic points for  $\text{Fe}^{\text{III}}$  and  $\text{Fe}^{\text{IV}}$  interconversions (353 and 400 nm) under pseudo-first-order conditions. The pseudo-first-order rate constant ( $k_{\text{obs}}$ ) calculated from the absorbance vs time traces at both wavelengths were obtained from nonlinear curve fitting  $[A_t = A_\infty - (A_\infty - A_0)e^{-(k_{\text{obs}}t)}]$  (Supporting Information Figures SI 8 and 9) and exhibited good agreement in rate constant values within 5% error. The  $k_{\text{obs}}$  values thus obtained correlated linearly with the substrate

concentration to provide the second order rate constant  $k_2$  (Supporting Information Figure SI 9), and it was observed that the rate constant decreased with an increase in the BDE of C–H bonds in the substrates. Linearity in Bell–Evans–Polanyi (BEP) relation was found from the plot of  $\log k_2'$  ( $k_2/\text{the number of equivalent H atoms}$ ) vs BDE (Figure 3)<sup>28</sup> for all the substrates from cyclohexane to cumene (slope of  $-0.17$ ). This linearity supports hydrogen abstraction ( $\text{H}^\bullet$ ) from a C–H bond by  $\text{Fe}^{\text{V}}(\text{O})$  group of **2** in the r.d.s as has been previously reported for  $[\text{Fe}^{\text{IV}}(\text{O})(\text{N}_4\text{Py})(\text{CH}_3\text{CN})]$  complexes.<sup>29</sup> A significant kinetic isotope effect (KIE) of 9 was observed for toluene/toluene- $d_8$  at 25 °C, supporting the conclusion that the r.d.s entails abstraction of an H atom from the C–H bond by the  $\text{Fe}^{\text{V}}(\text{O})$  (Figure 3, inset); KIEs of 2.1 and 6.5 have been found for typical porphyrin  $\pi$ -radical cation  $[(4\text{-TMPyP})^{\bullet+} \text{Fe}^{\text{IV}}(\text{O})]^+$  and  $[(\text{TMP})^{\bullet+} \text{Fe}^{\text{IV}}(\text{O})(p\text{-CH}_3\text{-PyO})]^+$  with xanthene and xanthene- $d_2$ , respectively.<sup>9,29,30</sup> Oxygen incorporation from  $\text{Fe}^{\text{V}}(\text{O})$  into the cyclohexane was followed by using 55%  $\text{O}^{18}$  labeled  $\text{Fe}^{\text{V}}$ , which resulted 35%  $\text{O}^{18}$  enriched product, supporting a rebound mechanism. (Supporting Information Figure SI 7).

Thus, the data supports the conclusion that the mechanism of C–H activation by **2** involves initial abstraction of an H atom from the hydrocarbon substrate by  $\text{Fe}^{\text{V}}(\text{O})$  followed by rebound to yield the oxidized product together with the regeneration of the parent  $\text{Fe}^{\text{III}}$  complex **1** (see Figure 3A and Supporting Information Figure SI 10 for pictorial representations of the proposed mechanism). The  $\text{Fe}^{\text{III}}$  complex **1** thus formed undergoes rapid comproportionation (Supporting Information Figure SI 4) with **2** to form the observed  $\mu$ -oxo- $(\text{Fe}^{\text{IV}})_2$  product (UV-vis,  $^1\text{H}$  NMR). Kinetic studies of the comproportionation reaction between **2** and **1** show that the second order rate constant ( $1.00 \times 10^5 \text{ M}^{-1}\text{s}^{-1}$ ; see Supporting Information Figure SI 4) is at least  $10^5$ -fold faster than the rate for C–H activation. Because this comproportionation reaction is extremely fast, the direct conversion of **2** to **1** is not observed in initial spectral scans. This is also corroborated by the observation that the product formation in all the reactions is less than 50% for all the substrates. Similar observations have been reported for sulfide oxidation by the parent  $\text{Fe}^{\text{V}}(\text{O})$  TAML activator. However, in this system, the likely  $(\text{Fe}^{\text{IV}})_2\text{O}$  product formed by reacting **2** and **1** undergoes further slow reduction to finally yield **1**. The faster self-reduction of our  $\text{Fe}^{\text{IV}}$  species is in contrast to the prototype  $\text{Fe}$ -TAML system, where the  $\mu$ -oxo- $(\text{Fe}^{\text{IV}})_2$  is extremely stable and does not undergo reduction. Because the  $\text{Fe}^{\text{IV}}$  species is not reactive toward oxidation of alkanes, the formation of the oxidized product in the reaction is solely due to the reaction of alkanes with **2**. Preliminary experiments performed in the presence of  $\text{O}_2$  show high amounts of ketone formation in respect to the corresponding alcohol, indicating that the radical formed after C–H abstraction is capable of reacting with  $\text{O}_2$ , as has been proposed before.<sup>30</sup>

**Table 1. Summary of Data for the Oxidation of Different Hydrocarbon by  $\text{Fe}^{\text{V}}(\text{O})$**

alkane (no. of equivalent H atom)	$\text{BDE}_{\text{C-H}}$ (kcal $\text{mol}^{-1}$ )	$k_2$ ( $\text{M}^{-1} \text{s}^{-1}$ )	products (equiv/Fe)	conversion
$\text{PhCH}(\text{CH}_3)_2$ (1)	84.5	$(7.91 \pm 0.09) \times 10^{-1}$	$\text{PhC}(\text{OH})(\text{CH}_3)_2$ (0.49); $\text{PhC}(\text{O})\text{CH}_3$ (0.07)	56%
$\text{PhEt}$ (2)	87	$(2.84 \pm 0.21) \times 10^{-1}$	$\text{PhCH}(\text{OH})\text{CH}_3$ (0.3); $\text{PhC}(\text{O})\text{CH}_3$ (0.22)	52%
$\text{PhCH}_3$ (3)	90	$(1.36 \pm 0.16) \times 10^{-1}$	$\text{PhCHO}$ (0.30)	30%
2,3-dimethylbutane (2)	96.5	$(3.50 \pm 0.10) \times 10^{-2}$	2,3-dimethyl-2-butanol (0.46)	46%
Cyclohexane (12)	99.3	$(2.26 \pm 0.10) \times 10^{-2}$	$\text{C}_6\text{H}_{11}\text{OH}$ (0.4); $\text{C}_6\text{H}_{10}\text{O}$ (0.02)	42%



In conclusion, we have successfully synthesized an  $\text{Fe}^{\text{V}}(\text{O})$  complex of a biuret-containing TAML activator at room temperature. EPR and Mössbauer spectroscopic studies show quantitative conversion of  $\text{Fe}^{\text{III}}$  (**1**) to the  $\text{Fe}^{\text{V}}(\text{O})$  complex. This complex displays remarkably higher stability at room temperature than any previously reported  $\text{Fe}^{\text{V}}\text{-oxo}$  complex. This higher stability has allowed us to study oxidation reactions with alkanes having strong C–H bond, such as that in cyclohexane ( $\text{BDE}_{\text{C-H}} = 99.3 \text{ kcal mol}^{-1}$ ), at room temperature. This is the first report of a well-defined  $\text{Fe}^{\text{V}}(\text{O})$  species that has been shown to react with strong C–H bonds. It was observed that **2** oxidizes cyclohexane to cyclohexanol and cyclohexanone with high reaction rates,  $k_2$  at  $25^\circ\text{C}$  is  $(2.26 \pm 0.10) \times 10^{-2} \text{ M}^{-1} \text{ s}^{-1}$  (Supporting Information Figure SI 9).<sup>31</sup> It is possible that the subsequent oxygen atom incorporation may proceed by either rebound mechanism or a dissociative mechanism or a combination of both, as has been recently proposed.<sup>32</sup> Studies aimed at further understanding the complete reaction mechanism including efforts to crystallographically characterize **2** are underway.

## ■ ASSOCIATED CONTENT

### ■ Supporting Information

Experimental details, characterization data, details of kinetic studies and proposed mechanism. This material is available free of charge via the Internet at <http://pubs.acs.org>.

## ■ AUTHOR INFORMATION

### Corresponding Authors

\*E-mail: [ss.sengupta@ncl.res.in](mailto:ss.sengupta@ncl.res.in). Fax: +91 2590 2621. Tel: +91 2590 2747. (S. Sen Gupta)

\*E-mail: [bb.dhar@ncl.res.in](mailto:bb.dhar@ncl.res.in). Tel: +91 2590 3207. (B. B. Dhar)

### Notes

The authors declare no competing financial interest.

## ■ ACKNOWLEDGMENTS

S.S.G. acknowledges DAE (BRNS; Grant no 2009/37/33/BRNS) for funding. M.G., K.K.S, and C.P. acknowledge CSIR (Delhi) for fellowships. B.B.D. also acknowledges CSIR for a SRA position. S.S.G. and M.G. thank Dr. A. Ryabov for discussion. S.S.G. thanks Dr. Nandini Devi, Dr. Amol Kulkarni and Dr. H. V. Thulasiram for help with UV–vis, GC and GC–MS.

## ■ REFERENCES

- (1) Costas, M.; Mehn, M. P.; Jensen, M. P.; Que, L. *Chem. Rev.* **2004**, *104*, 939–986.
- (2) Meunier, B.; de Visser, S. I. P.; Shaik, S. *Chem. Rev.* **2004**, *104*, 3947–3980.
- (3) Que, L.; Tolman, W. B. *Nature* **2008**, *455*, 333–340.
- (4) Rittle, J.; Green, M. T. *Science* **2010**, *330*, 933–937.
- (5) Solomon, E. I.; Brunold, T. C.; Davis, M. I.; Kemley, J. N.; Lee, S.-K.; Lehnert, N.; Neese, F.; Skulan, A. J.; Yang, Y.-S.; Zhou, J. *Chem. Rev.* **1999**, *100*, 235–350.
- (6) Ortiz de Montellano, P. R. *Chem. Rev.* **2009**, *110*, 932–948.
- (7) Price, J. C.; Barr, E. W.; Glass, T. E.; Krebs, C.; Bollinger, J. M. J. *Am. Chem. Soc.* **2003**, *125*, 13008–13009.
- (8) Price, J. C.; Barr, E. W.; Tirupati, B.; Bollinger, J. M.; Krebs, C. *Biochemistry* **2003**, *42*, 7497–7508.
- (9) Bell, S. R.; Groves, J. T. *J. Am. Chem. Soc.* **2009**, *131*, 9640–9641.
- (10) Klinker, E. J.; Kaizer, J.; Brennessel, W. W.; Woodrum, N. L.; Cramer, C. J.; Que, L. *Angew. Chem., Int. Ed.* **2005**, *44*, 3690–3694.
- (11) Xue, G.; Wang, D.; De Hont, R.; Fiedler, A. T.; Shan, X.; Münck, E.; Que, L. *Proc. Natl. Acad. Sci. U. S. A.* **2007**, *104*, 20713–20718.
- (12) Collins, T. J.; Khetan, S. K.; Ryabov, A. D. Iron-TAML catalysts in green oxidation processes based on hydrogen peroxide. In *Handbook of Green Chemistry*; Anastas, P., Crabtree, R., Eds.; Wiley-VCH: Weinheim, 2009; pp 39–77.
- (13) Ryabov, A. D.; Collins, T. J. *Adv. Inorg. Chem.* **2009**, *61*, 471–521.
- (14) Fukuzumi, S.; Morimoto, Y.; Kotani, H.; Naumov, P. e.; Lee, Y.-M.; Nam, W. *Nat. Chem.* **2010**, *2*, 756–759.
- (15) Que, L. *Acc. Chem. Res.* **2007**, *40*, 493–500.
- (16) Rohde, J.-U.; In, J.-H.; Lim, M. H.; Brennessel, W. W.; Bukowski, M. R.; Stubna, A.; Münck, E.; Nam, W.; Que, L. *Science* **2003**, *299*, 1037–1039.
- (17) Chow, T. W.-S.; Wong, E. L.-M.; Guo, Z.; Liu, Y.; Huang, J.-S.; Che, C.-M. *J. Am. Chem. Soc.* **2010**, *132*, 13229–13239.
- (18) Prat, I.; Mathieson, J. S.; Güell, M.; Ribas, X.; Luis, J. M.; Cronin, L.; Costas, M. *Nat. Chem.* **2011**, *3*, 788–793.
- (19) Lyakin, O. Y.; Bryliakov, K. P.; Britovsek, G. J. P.; Talsi, E. P. *J. Am. Chem. Soc.* **2009**, *131*, 10798–10799.
- (20) McDonald, A. R.; Que, L. *Nat. Chem.* **2011**, *3*, 761–762.
- (21) Van Heuvelen, K. M.; Fiedler, A. T.; Shan, X.; De Hont, R. F.; Meier, K. K.; Bominaar, E. L.; Münck, E.; Que, L. *Proc. Natl. Acad. Sci. U. S. A.* **2012**, *109*, 11933–11938.
- (22) de Oliveira, F. T.; Chanda, A.; Banerjee, D.; Shan, X.; Mondal, S.; Que, L.; Bominaar, E. L.; Münck, E.; Collins, T. J. *Science* **2007**, *315*, 835–838.
- (23) Kundu, S.; Thompson, J. V. K.; Ryabov, A. D.; Collins, T. J. *J. Am. Chem. Soc.* **2011**, *133*, 18546–18549.
- (24) (a) Panda, C.; Ghosh, M.; Panda, T.; Banerjee, R.; Sen Gupta, S. *Chem. Commun.* **2011**, *47*, 8016–8018. (b) Collins, T. J.; Gordon-Wylie, S. Long-Lived Homogeneous Oxidation Catalysts. U.S. Patent 5,847,120, December 8, 1998.
- (25) Collins, T. J. *Acc. Chem. Res.* **2002**, *35*, 782–790.
- (26) Bartos, M. J.; Gordon-Wylie, S. W.; Fox, B. G.; James Wright, L.; Weintraub, S. T.; Kauffmann, K. E.; Münck, E.; Kostka, K. L.; Uffelman, E. S.; Rickard, C. E. F.; Noon, K. R.; Collins, T. J. *Coord. Chem. Rev.* **1998**, *174*, 361–390.
- (27) Ghosh, A.; de Oliveira, F. T.; Yano, T.; Nishioka, T.; Beach, E. S.; Kinoshita, I.; Münck, E.; Ryabov, A. D.; Horwitz, C. P.; Collins, T. J. *J. Am. Chem. Soc.* **2005**, *127*, 2505–2513.
- (28) (a) Mayer, J. M. *Acc. Chem. Res.* **1998**, *31*, 441–450. (b) Bryant, J. R.; Mayer, J. M. *J. Am. Chem. Soc.* **2003**, *125*, 10351–10361.
- (29) Kaizer, J. z.; Klinker, E. J.; Oh, N. Y.; Rohde, J.-U.; Song, W. J.; Stubna, A.; Kim, J.; Münck, E.; Nam, W.; Que, L. *J. Am. Chem. Soc.* **2004**, *126*, 472–473.
- (30) Kim, C.; Dong, Y.; Que, L. *J. Am. Chem. Soc.* **1997**, *119*, 3635–3636.
- (31) Kang, Y.; Chen, H.; Jeong, Y. J.; Lai, W.; Bae, E. H.; Shaik, S.; Nam, W. *Chem.–Eur. J.* **2009**, *15*, 10039–10046.
- (32) Cho, K.-B.; Wu, X.; Lee, Y.-M.; Kwon, Y. H.; Shaik, S.; Nam, W. *J. Am. Chem. Soc.* **2012**, *134*, 20222–20225.